Parameters Identification for Motorcycle Simulator's Platform Characterization

Lamri Nehaoua, Hichem Arioui

Parameters Identification for Motorcycle Simulator's Platform Characterization ⋆

L. Nehaoua * **H. Arioui** **

* *Institut National de Recherche sur les Transports et leur Sécurité, INRETS, 2 Av Gl Malleret-Joinville, 94114, Arceuil, France (e-mail: nehaoua@inrets.fr).*
** *IBISC LSC-LAMI CNRS-FRE 2873, 40 rue Pelvoux 91020, Evry, France(e-mail: Hichem.Arioui@iup.univ-evry.fr).*

Abstract: This paper presents the dynamics modeling and parameters identification of a motorcycle simulator's platform. This model begins with some suppositions which consider that the leg dynamics can be neglected with respect to the mobile platform one. The objectif is to synthesis a simplified control scheme, adapted to driving simulation application, minimising dealys and without loss of tracking performance.
Electronic system of platform actuation is described. It's based on a CAN BUS communication which offers a large transmission robustness and error handling. Despite some disadvanteges, we adapted a control solution which overcome these inconvenients and preserve the quality of tracking trajectory.
A bref description of the simulator's platform is given and results are shown and justified according to our specifications.

1. INTRODUCTION

HUman applications are becoming more widespread in different areas of scientific research at the international level. This is for several reasons, in order to prevent hazardeous driving situations, learning novice drivers and detect behavioral anomalies (somnolence, drags,...etc). On the other hand, the context of road safety is an international problem and constitutes a daily struggle for different governments to reduce the number of accidents through prevention, as well as testing new systems of security and assistance.

Driving simulators were extensively used in the aeronautical and automotive areas. They present an inexpensive tools for training future bikers and develop new technological features. The main theories used in this area have been developed for flight simulation. However, the adaptation of these technologies to other simulators (cars and motorcycles) is possible by taking in care some characteristics of land vehicles. Indeed, their dynamics is more constrained and human - machine interaction is more rich. This situation is much more complicated for two-wheeled vehicles, minimization of risk and the lack of visibility leads to fatal consequences, while knowing that the power-mass ratio is more important.

Very little two-wheeled vehicles simulators are constructed comparing to those of cars. Main works were acheived by Honda, a leading manufacturer in the field of two-wheeled vehicles (Miyamaru et al. [2002]Chiyoda et al. [2000]). Honda has developed several prototypes from 1988, one of them has been heavily marketed, supported by a Japanese law demanding a few hours of riding simulation before awarding the motorcycle licence. PERCRO, a laboratory based in Italy, in the context of the MORIS project, have constructed a motorbike simulator based on a classical 6 degrees of freedom (DOF) Stewart platform (Ferrazzin et al. [2003]). Finally, a 5DOF simulator is designed in the Department of Mechanical Engineering at Padova University, espacially dedicated to the competition motorcycle (Cossalter et al. [2004]).

The main difficulty in developing a driving simulator is the choice of the mechanical platform engineering. The position of the different axes of rotation should be properly investigated in order to avoid false cues or unwanted motion. Actuation system is one of more important feature because it defines the simulator's bandwidth and hence, the motion frequency components that it can reproduce. The choice of electronic acquisition must be taken from a wide range of commercial or locally built solutions. Analog flow control offers best performances in spite of great vulnerability against noise measurements and sensors multiplication. Today, servocontrollers are more powerful and present digital solutions which are robust, requiring fewer sensors. The choice of a communication that facilitate the error management increase greatly the safety of subjects and thus satisfy one of the first requirements of the driving simulation.

2. PRELIMINARIES

The choice of the simulator architecture is guided by the necessary needs to have a sufficient perception during the riding simulation. Our goal is to reproduce the important inertial effects perceived for the application needs but not all the motorcycle movements. So, the real amplitude of the various DOF was not a dominating object during the design phase.

Based on these considerations, the number of degrees of freedom for our architecture is determined. We aim to develop a mechanical platform for training and behavioral study of two-wheeled vehicles users in a normal urban traffic and in situations of risk. Therefore, motorcycle dynamics is analyzed (Cossalter [2002]) in order to establish a precise specifications for the development of a first prototype (Figure 1). After several investigations, three movements were privileged:

⋆ This research was supported by funds from the NATIONAL RESEARCH AGENCY in SIMACOM project.

- Roll: is the most important mouvment for the reproduction of turns, slalom and lane change. Unlike car driving, the rider make an effort on handlebars to tilt his motorcycle. This inclination generates a gravity force that compensates the centrifugal one and thus help to keep the rider balance in turn. Other riding styles are also possible (riding with upper body inclination), these will not be taken into account in our first prototype.
- Pitch: this rotation allows to reproduce longitudinal accelerations present during acceleration and braking phases. This effect is vital for more realism of the riding simulation. Unlike speed which can be reproduced with the simple visual projection, acceleration can't be felt without body excitation via a mechanical motion. Special techniques called motion cueing algorithms can transform the actual motorcycle motion in an achievable movement by the simulator, which can create an acceleration illusion without causing sensory conflict (Nehaoua et al. [2007], Nehaoua et al. [2006]).
- Yaw: for slippage of the rear wheels in accident situations.

Fig. 1. Constructed riding motorcycle simulator

3. INVERSE KINEMATICS FORMULAION

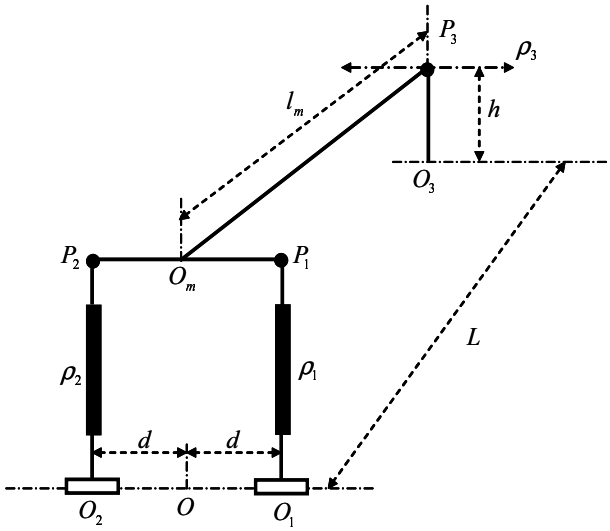

Fig. 2. Kinematics scheme of the simulator's platform

Let $\Re(O,i,j,k)$ be the fixed reference and $\Re_m(O_m,i_m,j_m,k_m)$ the platform mobile reference. O_1, O_2 and O_3 are repectively the attachment points of the two legs and the rear slide with the simulator's base. P_1, P_2 and P_3 are repectively the attachment points of the two legs and the rear slide with the upper mobile platform. The configuration of the reference frame $\Re_m$ is characterized by the position (x_m, y_m, z_m) of its origin point and the three Euler orientation angles (ψ, θ, φ), corresponding respectively to the yaw, pitch and roll angles. We take the Z-Y-X convention to compute the rotation matrix, as following:

$$R = R_\psi R_\theta R_\varphi = \begin{pmatrix} r_{11} & r_{12} & r_{13} \\ r_{21} & r_{22} & r_{23} \\ r_{31} & r_{32} & r_{33} \end{pmatrix} \tag{1}$$

or in a detailed form, where $c \equiv \cos$ and $s \equiv \sin$:

$$\mathbf{R} = \begin{pmatrix} c\theta c\psi & s\varphi s\theta c\psi - c\varphi s\psi & c\varphi s\theta c\psi + s\varphi s\psi \\ c\theta s\psi & s\varphi s\theta s\psi + c\varphi c\psi & c\varphi s\theta s\psi - s\varphi c\psi \\ -s\theta & s\varphi c\theta & c\varphi c\theta \end{pmatrix} \tag{2}$$

The vector $\mathbf{OP_3}$ is given in the fixed base reference by ${\mathbf{OP_3}}^O = (-L, \rho_3, h)^T$. Using the transformation matrix R the same vector can be written as following:

$${\mathbf{OP_3}}^O = {\mathbf{OO_m}}^O + R{\mathbf{O_mP_3}}^m \tag{3}$$

where, ${\mathbf{OO_m}}^O = (x_m, y_m, z_m)^T$ and ${\mathbf{O_mP_3}}^m = (-l_m, 0, 0)^T$. Replacing the different vectors components in equation (3) we can deduce the coordinates of the mobile reference origin O_m and the rear slide displacement ρ_3 such as:

$$\begin{cases} x_m = -L + l_m r_{11} \\ y_m = 0 \\ z_m = h - l_m r_{31} \\ \rho_3 = -l_m r_{21} \end{cases} \tag{4}$$

where L, h and l_m are geometric constants (figure 7).

Now, the leg vector equation for $i = 1, 2$ is:

$${\mathbf{O_iP_i}}^O = {\mathbf{O_iO}}^O + {\mathbf{OO_m}}^O + R{\mathbf{O_mP_i}}^m \tag{5}$$

where, ${\mathbf{O_mP_i}}^m = (0, (-1)^{i+1} l, 0)^T$, ${\mathbf{O_iO}}^O = (-1)^i d\mathbf{j}$ and d is the coordinate of the two cylindrical joints O_1 and O_2. l is the constant length between points P_1 and P_2. Replacing in equation (5) we can deduce the components of vectors ${\mathbf{O_iP_i}}^O = \rho_i u_i$ as following:

$$\rho_i \mathbf{u_i} = \begin{pmatrix} -L + l_m r_{11} + (-1)^{i+1} l r_{12} \\ 0 \\ h + l_m r_{31} + (-1)^{i+1} l r_{32} \end{pmatrix} \tag{6}$$

and

$$d = l r_{22} \tag{7}$$

where, $\mathbf{u_i}$ is the unit vector along the leg axis and $\rho_i^2 = {\mathbf{O_iP_i}}^T \mathbf{O_iP_i}$ are the legs lengths.

To determine the inverse Jacobian matrix, we note the Euler angle rates vector by $\dot{\mathbf{q}}_\mathbf{r} = (\dot\psi, \dot\theta, \dot\varphi)^T$. The velocity of the leg elongation is given by:

$$\dot\rho_i = \dot{\mathbf{O_iP_i}}^T \mathbf{u_i} \tag{8}$$

Deriving equation (5) and replacing in (8) we find that:

$$\dot\rho_i = (-1)^i {\mathbf{u_i}}^T d\mathbf{j} + {\mathbf{u_i}}^T . \mathbf{O\dot O_m} + (\Omega \times \mathbf{O_mP_i})^T \mathbf{u_i} \tag{9}$$

where $\Omega = \gamma \dot{\mathbf{q}}_\mathbf{r}$ is the mobile platform angular velocity expressed in the fixed reference frame, and γ is the matrix

transformation between the angular velocities and Euler rates. Equation (9) can be written using the property of the mixed vector product $(\mathbf{u}\times\mathbf{v}).\mathbf{w}=(\mathbf{w}\times\mathbf{u}).\mathbf{v}$ as following:

$$\dot{\rho}_i=(-1)^i\mathbf{u_i}^T\dot{d}\mathbf{j}+\mathbf{u_i}^T.\mathbf{O}\dot{\mathbf{O}}_\mathbf{m}+(\mathbf{u_i}\times\mathbf{P_iO_m})^T\Omega \quad (10)$$

For the rear slide velocity, we derive the equation of $\rho_3=\mathbf{j}^T\mathbf{O}\dot{\mathbf{P}}_\mathbf{3}$. Rearranging, we obtain:

$$\dot{\rho}_3=\mathbf{j}^T\mathbf{O}\dot{\mathbf{O}}_\mathbf{m}+(\mathbf{j}\times\mathbf{P_3O_m})^T\boldsymbol{\Omega} \quad (11)$$

From equations (10) and (11) and knowing that $\mathbf{u_i}^T\mathbf{j}=0$, we can deduce that:

$$\rho=J_{-1}W \quad (12)$$

where, $\rho=(\rho_1,\rho_2,\rho_3)^T$, $W=(\mathbf{O}\dot{\mathbf{O}}_\mathbf{m},\dot{\mathbf{q}}_\mathbf{r})^T$ and the inverse Jacobian is:

$$J_{-1}=\begin{bmatrix}\mathbf{u_1}^T & (\mathbf{u_1}\times\mathbf{P_1O_m})^T\\ \mathbf{u_2}^T & (\mathbf{u_2}\times\mathbf{P_2O_m})^T\\ \mathbf{j}^T & (\mathbf{j}\times\mathbf{P_3O_m})^T\end{bmatrix} \quad (13)$$

The platform is designed to perform three rotations of $\pm15°$, The inverse Jacobian matrix is always invertible within this domain, so there is no singularity of the platform within its workspace.

4. DYNAMICS OF THE PLATFORM

In this section, a simple dynamics formulation of the simulator's platform will be demonstrated. The main objective is to propose a control scheme adapted for our riding application and, to characterize the platform capabiities. For this, we neglete at first time the contribution of legs dynamics and we focus on the upper platform motion. Applying Newton-Euler equations on the mobile platform gives (Dasgupta and Mruthyunjaya [1998]):

$$\begin{array}{l}m_p\mathbf{g}+\mathbf{F}_1+\mathbf{F}_2+\mathbf{F}_3=m_p\ddot{\mathbf{O}\mathbf{G}}_p\\ m_p\mathbf{O_mG_p}\times\mathbf{g}+\mathbf{O_mP_1}\times\mathbf{F}_1+\mathbf{O_mP_2}\times\mathbf{F}_2+\\ \mathbf{O_mP_3}\times\mathbf{F}_3=m_p\mathbf{O_mG_p}\times\ddot{\mathbf{O}\mathbf{G}}_p+\mathbf{I_p}\dot{\Omega}+\Omega\times\mathbf{I_p}\Omega\end{array} \quad (14)$$

where $\mathbf{F_i}$, $i=1..3$ are actuation forces of the front two legs and rear slide. m_p, $\mathbf{I_p}$ platform masse and inertia matrix. $\mathbf{O_mG_p}$ position of the mobile platform center of gravity G_p with respect to point O_m. All vectors and matrices are expressed in the global reference frame (O,i,j,k). Ω is the rotational velocity yet expressed in the inverse kinematics section. Combining the two equations into one algebraic formulation:

$$\mathbf{J}_{-1}^T\mathbf{F}=m_p\begin{bmatrix}\mathbf{I_3}\\ \widetilde{\mathbf{O_mG_p}}\end{bmatrix}(\ddot{\mathbf{O}\mathbf{G}}_p-\mathbf{g})+\begin{bmatrix}\mathbf{0_{3\times1}}\\ \mathbf{I_p}\dot{\Omega}+\Omega\times\mathbf{I_p}\Omega\end{bmatrix} \quad (15)$$

with $\mathbf{I_3}$ is 3×3 identity matrix, $\mathbf{F}=[\,\mathbf{F_1}\ \mathbf{F_2}\ \mathbf{F_3}\,]^T$, $\mathbf{0_{3\times1}}=[\,0\ 0\ 0\,]^T$ and $\mathbf{J}_{-1}$ is the inverse jacobian matrix. $\ddot{\mathbf{O}\mathbf{G}}_p$ is the acceleration of the platform center of gravity with respect to global frame given by:

$$\ddot{\mathbf{O}\mathbf{G}}_p=\ddot{\mathbf{O}\mathbf{O}}_m+\dot{\Omega}\times\mathbf{O_mG}_p+\Omega\times(\Omega\times\mathbf{O_mG}_p) \quad (16)$$

We Note $W=(\mathbf{O}\dot{\mathbf{O}}_\mathbf{m},\Omega)^T$ the platform wrench. Then, $\ddot{\mathbf{O}\mathbf{G}}_p$ can be written in more convenient equation as:

$$\ddot{\mathbf{O}\mathbf{G}}_p=\begin{bmatrix}\mathbf{I_3} & -\widetilde{\mathbf{O_mG_p}}\end{bmatrix}\dot{\mathbf{W}}+\widetilde{\Omega}^2\mathbf{O_mG_p} \quad (17)$$

where $\widetilde{\Omega}$ is the skew matrix of vector Ω given by:

$$\widetilde{\Omega}=\begin{pmatrix}0 & -\Omega_3 & \Omega_2\\ \Omega_3 & 0 & -\Omega_1\\ -\Omega_2 & \Omega_1 & 0\end{pmatrix} \quad (18)$$

Replacing in equation (17) into (15) and with some algebraic manipulations we deduce the simplified dynamic model of the simulator's platform as:

$$\mathbf{M}\dot{\mathbf{W}}+\mathbf{C}+\mathbf{G}=\mathbf{J}_{-1}^T\mathbf{F} \quad (19)$$

where, $\mathbf{M}$ is mass matrix, $\mathbf{C}$ is a nonlinear vector function of the angular velocity and $\mathbf{G}$ is the gravity term given as following:

$$\mathbf{M}=\begin{bmatrix}m_p\mathbf{I_3} & -m_p\widetilde{\mathbf{O_mG_p}}\\ m_p\widetilde{\mathbf{O_mG_p}} & \mathbf{I_p}-m_p\widetilde{\mathbf{O_mG_p}}^{\,2}\end{bmatrix} \quad (20)$$

$$\mathbf{C}=\begin{bmatrix}m_p\widetilde{\Omega}^2\mathbf{O_mG_p}\\ \widetilde{\Omega}\mathbf{I_p}\Omega+m_p\widetilde{\mathbf{O_mG_p}}\widetilde{\Omega}^2\mathbf{O_mG_p}\end{bmatrix} \quad (21)$$

$$\mathbf{G}=-m_p\begin{bmatrix}\mathbf{I_3}\\ \widetilde{\mathbf{O_mG_p}}\end{bmatrix}\mathbf{g} \quad (22)$$

At this point, this model is convenient for describing the dynamics of fully actuated 6DOF platform. However, our architecture is a 3DOF where the three rotations and the three translation are dependent. Then, we must include three algebraic constraint equations. A simple formulation of Lagrange multiplyers is added to the model formula as:

$$\mathbf{M}\dot{\mathbf{W}}+\mathbf{C}+\mathbf{G}+\Phi_q^T\lambda=\mathbf{J}_{-1}^T\mathbf{F} \quad (23)$$

with, Φ_q is the jacobian of the constraint matrix $\Phi(q,t)$ and λ are the Lagrange multiplyers. Due to the symmetrical representation of the machanical platform, the algebraic constraints can be deduced from the coordinates expression of the vector $\mathbf{OO_m}=(x_m,y_m,z_m)^T$, so:

$$\Phi(q,t)=\begin{cases}x_m+L-l_3c\theta c\psi-h_3(c\varphi s\theta c\psi+s\varphi s\psi)=0\\ y_m=0\\ z_m-h+l_3s\theta-h3c\varphi c\theta=0\end{cases} \quad (24)$$

By derivation with respect to time variable, it results that $\dot{\Phi}(q,t)=\Phi_q\mathbf{W}$, where:

$$\Phi_q=\begin{bmatrix}1&0&0&q_1&q_2&q_3\\ 0&1&0&0&0&0\\ 0&0&1&0&q_4&q_5\end{bmatrix} \quad (25)$$

and:

$$\begin{cases}q_1=l_3c\theta s\psi+h_3(c\varphi s\theta s\psi-s\varphi c\psi)\\ q_2=l_3s\theta c\psi-h_3c\varphi c\theta c\psi\\ q_3=h_3s\varphi s\theta c\psi-h_3c\varphi s\psi\\ q_4=l_3c\theta+h_3c\varphi s\theta\\ q_5=h_3s\varphi c\theta\end{cases} \quad (26)$$

Knowing that $\mathbf{O}\dot{\mathbf{O}}_\mathbf{m}=\Gamma\dot{\mathbf{q}}$, $\Omega=\gamma\dot{\mathbf{q}}$, then $\mathbf{W}=\mathbf{A}\dot{\mathbf{q}}$ and $\dot{\mathbf{W}}=\mathbf{A}\ddot{\mathbf{q}}+\dot{\mathbf{A}}\dot{\mathbf{q}}$, where $\mathbf{A}=[\,\Gamma\ \gamma\,]^T$, we can deduce a reduced representation of the dynamics model such:

$$\mathbf{M}'\ddot{\mathbf{q}}+\mathbf{C}'+\mathbf{G}=\mathbf{J}_{-1}^T\mathbf{F}-\Phi_q^T\lambda \quad (27)$$

where $\mathbf{M}'=\mathbf{MA}$, $\mathbf{C}'=\mathbf{M}\dot{\mathbf{A}}\dot{\mathbf{q}}+\mathbf{C}$ and $\mathbf{q}=(\psi,\theta,\varphi)$.

5. IDENTIFICATION

In this section, we expose an identification procedure to estimate the mass and inertia parameters. For this, the dynamics model must be written in linear form with respect to different parameters to be estimated. A simple manner to achieve this, is to express the dynamics model in the local frame of the upper platform, where the inertia matrix is constant. In the present work, we will continu with the previous formulation in the global frame, because we intend in the next works to extend this procedure to identify the whole platform parameters using a more complex model, which include the legs dynamics. From equation (15):

$$\mathbf{J}_{-1}^{T}\mathbf{F} - \Phi_q^T\lambda = m_p \begin{bmatrix} \mathbf{I_3} \\ \widetilde{\mathbf{O_m G_p}} \end{bmatrix} (\ddot{\mathbf{OG}}_p - \mathbf{g}) + \begin{bmatrix} \mathbf{0_{3\times 1}} \\ \mathbf{I_p}\dot{\Omega} + \Omega \times \mathbf{I_p}\Omega \end{bmatrix} \tag{28}$$

Matrix inertia in the global frame is function of the platform configuration such, $\mathbf{I_p} = \mathbf{R}\mathbf{I_0}\mathbf{R}^T$, where $\mathbf{I_0}$ is the constant inertia matrix of the platform about its center of gravity, supposed diagonal in a first approximation. So:

$$\mathbf{I_p} = \begin{bmatrix} r_{11} & r_{12} & r_{13} \\ r_{21} & r_{22} & r_{23} \\ r_{31} & r_{32} & r_{33} \end{bmatrix} \begin{bmatrix} I_1 & 0 & 0 \\ 0 & I_2 & 0 \\ 0 & 0 & I_3 \end{bmatrix} \begin{bmatrix} r_{11} & r_{21} & r_{31} \\ r_{12} & r_{22} & r_{32} \\ r_{13} & r_{23} & r_{33} \end{bmatrix} \tag{29}$$

Simplifying, we can deduce a linear formulation of $\mathbf{I_p}$ such that $\mathbf{I_p} = \mathbf{R_1}I_1 + \mathbf{R_2}I_2 + \mathbf{R_3}I_3$, where:

$$\mathbf{R_1} = \begin{bmatrix} r_{11}^2 & r_{11}r_{12} & r_{11}r_{13} \\ r_{11}r_{21} & r_{21}^2 & r_{21}r_{31} \\ r_{11}r_{31} & r_{21}r_{31} & r_{31}^2 \end{bmatrix} \tag{30}$$

$$\mathbf{R_2} = \begin{bmatrix} r_{12}^2 & r_{12}r_{22} & r_{12}r_{32} \\ r_{12}r_{22} & r_{22}^2 & r_{22}r_{32} \\ r_{12}r_{32} & r_{22}r_{32} & r_{32}^2 \end{bmatrix} \tag{31}$$

$$\mathbf{R_3} = \begin{bmatrix} r_{13}^2 & r_{13}r_{23} & r_{13}r_{33} \\ r_{13}r_{23} & r_{23}^2 & r_{23}r_{33} \\ r_{13}r_{33} & r_{23}r_{33} & r_{33}^2 \end{bmatrix} \tag{32}$$

Replacing this in the last term of equation (28) yeilds:

$$\begin{bmatrix} \mathbf{0_{3\times 1}} \\ \mathbf{I_p}\dot{\Omega} + \Omega \times \mathbf{I_p}\Omega \end{bmatrix} = \mathbf{R_1}''I_1 + \mathbf{R_2}''I_2 + \mathbf{R_3}''I_3 \tag{33}$$

where, $\mathbf{R_i}'' = \begin{bmatrix} \mathbf{0_{3\times 1}} & \mathbf{R_i}' \end{bmatrix}^T$ and $\mathbf{R_i}' = \mathbf{R_i}\dot{\Omega} + \widetilde{\Omega}\mathbf{R_i}\Omega$

Finally, the dynamics model can be written in a linear formulation of the different parameters as following:

$$\Phi_p\mathbf{p} = \mathbf{J}_{-1}^T\mathbf{F} \tag{34}$$

with $\Phi_p = \begin{bmatrix} \mathbf{M_g} & \mathbf{R_1}'' & \mathbf{R_2}'' & \mathbf{R_3}'' & \Phi_q \end{bmatrix}$, $\mathbf{p} = [\, m_p \;\; I_1 \;\; I_2 \;\; I_3 \;\; \lambda \,]$ and $\mathbf{M_g} = \begin{bmatrix} \mathbf{I_3} & \widetilde{\mathbf{O_m G_p}} \end{bmatrix}^T (\ddot{\mathbf{OG}}_p - \mathbf{g})$.

Next, several methods were developped in litterature for the parametric identification. We choose the adaptive gradient method due to its simplicity in an off-line or an online implementation. Then, if $\tau = \mathbf{J}_{-1}^T\mathbf{F}$ this method consist at optimizing a quadratic cost function $\mathbf{J} = 1/2(\tau_{ref} - \tau)^2$, where τ_{ref} relates to measured actuation torques. Adaptation law is expressed as following:

$$\dot{\mathbf{p}} = -\mathbf{K}\frac{\partial \mathbf{J}}{\partial \mathbf{p}} \tag{35}$$

where $\mathbf{K}$ is adaptation matrix coefficient, ajusted to ensure rapid convergence and are also lied to the different excitation trajectories (slow or rapid reference trajectory). Finally, the different paramterts are obtained by integrating the following equation:

$$\dot{\mathbf{p}} = \mathbf{K}\Phi_p^T(\tau_{ref} - \Phi_p\mathbf{p}) \tag{36}$$

6. EXPERIMENTATION

6.1 Actuation system

Simulator's platform is electrically actuated. The front two legs are lead-secrew type driven by a Parker Hannifin SMBAB6045 brushless servomotor and a Lust CDD3000 servocontroller. The rear slide is actuated by an SMBAB82300 brushless servomotor coupled with Tecnoingranaggi MP060.1.10 reductor. The different servocontrollers offer a various Preset solutions to drive the platform (in position, velocity or torque scheme) and are equipped with CAN (Controller Area Network) modules for digital transmission. This constitutes a robust solution against noise and offers a big simplicity for the task management and errors handling. More, with CAN modules we can acquire position, velocity, actual torque and phase current without installing more sensors. This is a very flexible solution but it prensents three major disadvantages:

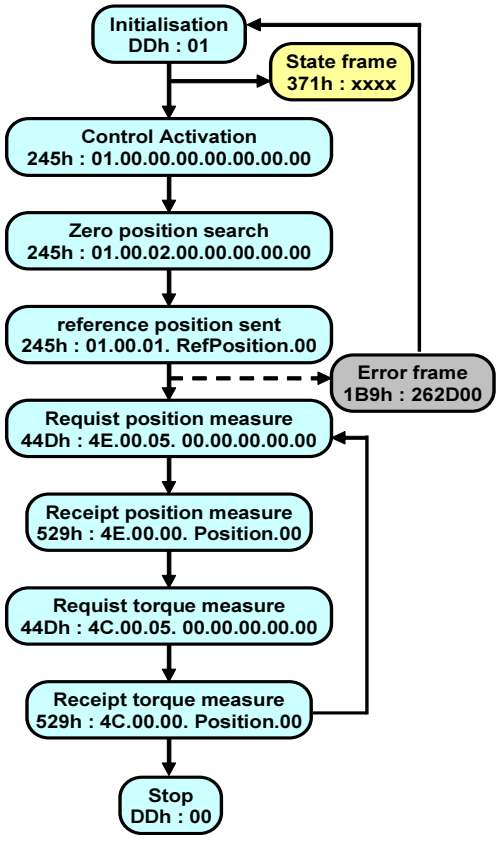

Fig. 3. CAN frames organization: for exemple initialisation is done by a frame with identifier 0DD (in hexa). An error frame resulting from course limitation is sent with an identifier 1B9

(1) all parameters (position, velocity, actual torque and phase current) are codded on the same CAN frame and hence, a parallel acquisition is not possible (constructor limitation)

(2) parameter channel is treated with low priority and every requist and response CAN frame is fixed at 10ms (to acquire just one measure of position and torque, we must send two request frames and receipt two responses frame which present 20ms, figure 3)
(3) Comparing to analog flow control, this solution present some delays related to the computing time of the servocontroller and the transmission delays.

For our riding simulator application, such delays may creat a serious problems and contribute to the generation of the simulator's sickness. To overcome this limitations, and knowing that in driving simulation, delays minisation is more important than an accurate trajectory tracking, we have optimized the inner servocontroller control scheme without using an externel control loop.

6.2 Control

We aim to explore the capabilities of two control methods, the first based on torque computing scheme, which need a good parameters identification. The second controller based on the optimisation of the inner control loop of the servocontroller to satisfy prior specifications (acceptable tracking error and sufficient stability margins).

Torque computing method allows the compensation of gravity and nonlinear terms with a feedforward term, as:

$$\tau = \tau_{ff} + \tau_{fb} = (\mathbf{M}'\ddot{\mathbf{q}}_\mathbf{d} + \mathbf{C}' + \mathbf{G}) + \mathbf{M}'(\mathbf{K_p}\mathbf{e} + \mathbf{K_d}\dot{\mathbf{e}}) \quad (37)$$

where $\mathbf{e} = \mathbf{q_d} - \mathbf{q}$ is the tracknig error. $\mathbf{K_p}$, $\mathbf{K_d}$ are gain matrices to be adjusted. Remplacing torque τ in the equation of the dynamics model gives:

$$\mathbf{M}'\ddot{\mathbf{q}} + \mathbf{C}' + \mathbf{G} = (\mathbf{M}'\ddot{\mathbf{q}}_\mathbf{d} + \mathbf{C}' + \mathbf{G}) + \mathbf{M}'(\mathbf{K_p}\mathbf{e} + \mathbf{K_d}\dot{\mathbf{e}}) \quad (38)$$

Then:

$$\ddot{\mathbf{e}} + \mathbf{K_p}\mathbf{e} + \mathbf{K_d}\dot{\mathbf{e}} = 0 \quad (39)$$

which means that $\mathbf{K_p}$, $\mathbf{K_d}$ can be adjusted by a classical control method such pole placement.

For the second method, each servocontroller contains three inner control loops, a Proportionnel position loop and two proportionnal-Integral loops for speed and current control. A pre-control solution is also implemented to compensate for external load inertia and friction by a prediction of articulation velocity and acceleration (figure 4).

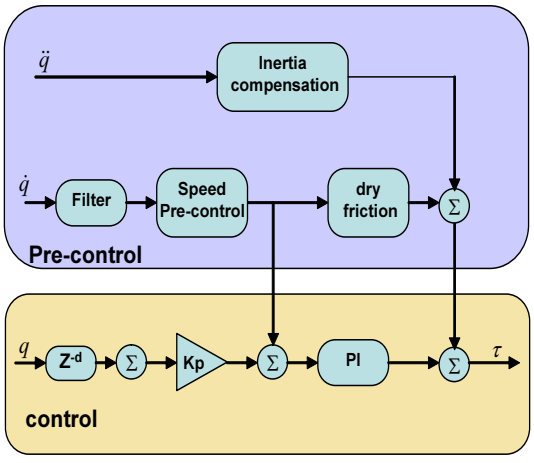

Fig. 4. Servocontroller inner control loops

Figure 5 presents the measured legs displacement for a step reference of $1cm$. It is shown that the performance of the computed torque method is better than of that obtained by the servocontroller loops. However, for our application, this is sufficient with a great advantage of reducing communications delays and time computing. An additional effort may be made to better optimize the Proportionnel and PI parameters of servo inner loops control. Noting that, in this experimentation, the precontrol part is disabled and this, carrefully used, may greatly increase control performances.

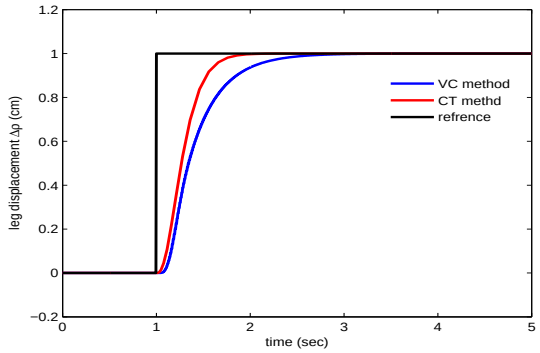

Fig. 5. Measured legs displacement for a step reference. (VC):using servocontroller control loops. (CT): using computing torque method

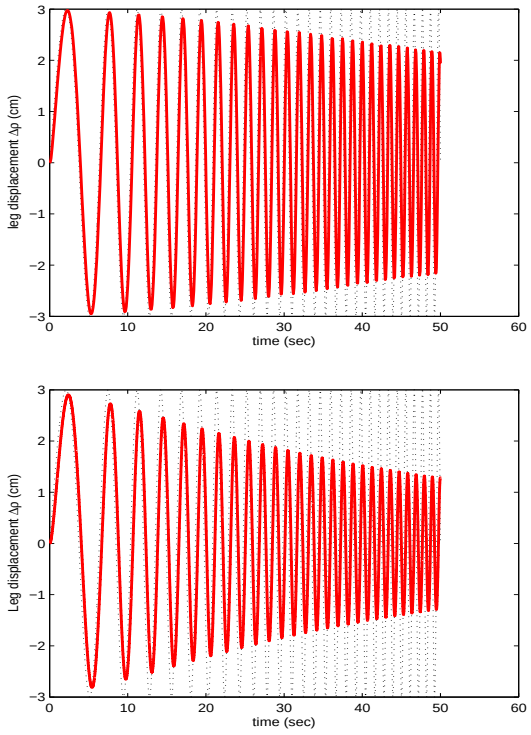

Fig. 6. Measured legs displacement for a chirp sine reference. (a): using computing torque method. (b):using servocontroller control loops.

Figure 6 shows the measured legs displacement for a chirp sine reference displacement with a variable frequency. Computed torque method allows more bandwith than the second method,

this represents an important feature in driving simulation. Transitory components of motorcycle motion are difficult to reproduce with our simulator platform. These components are in the range of 3-5Hz, and are mainly used to reproduce an illusion of acceleration and braking. For this, psychophysical experimentation will be conducted to validate the simulator applicability in a motorcycle riding view point, and hence, propose different solutions for the next prototype.

6.3 Identification

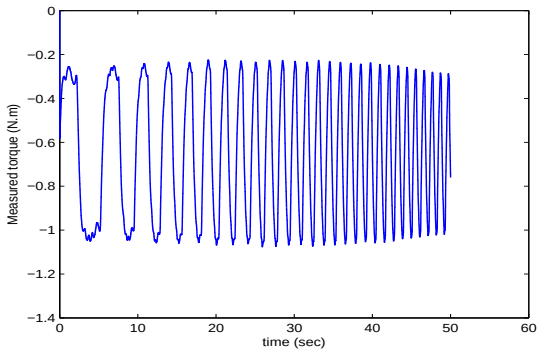

Fig. 7. Mesured leg torque

Figure 7 shows the measured torque corresponding to the chirp sine reference displacement of figure 6. Velocity and acceleration are obtained by numerical derivation. All variables are saved for un an off-line estimation procedure. Each DOF is separalty actuated in order to excit matrix inertia element by element. Adaptation gains are tuned by trail-error to have a fast convergence and according to the amplitude and frequency of excitation trajectory. Finally, identified parameters are presented in figure 8.

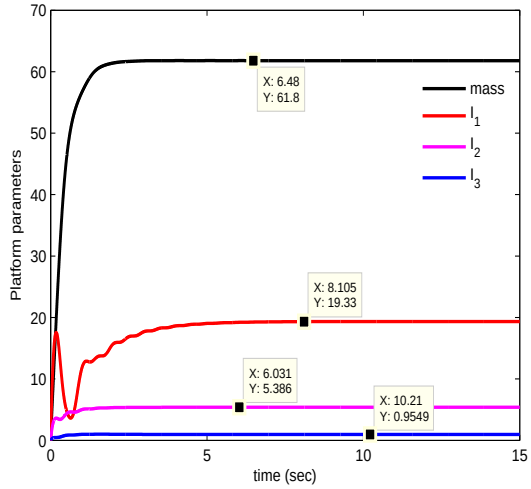

Fig. 8. Identified platform parameters

7. CONCLUSION

In the first part of this paper, the important points for the development of a riding simulator are exposed. We have justified the choice of the platform architecture and the actuation system to drive the different servomotors. Next, The inverse kinematics of the platform was presented allowing to transform the motion cueing algorithm trajectories into actuator inputs. Also, a detailed dynamics modeling of the simulator's platform is developed, based on some simplification. Algebraic constraints equations are included and a reduced representation of the dynamics model is demonstrated. An identification method is detailed which allows to estimate the platform parameters and to get a linear form of the dynamics model without re-writting it in a local reference frame.

Experiments were conducted to the present platform. A robust and powerfull electronic solution is described and a comparison between two control strategies is done. The main problems are high-lighted and adapted solutions are proposed to minimise delays and overcome the different limitations. Results are very sufficient for our riding simulation application.

Future work will be focus on the inclusion of the dynamics model into servocontroller parameters optimisation. Indeed, Proportionnel and PI control loops are optimized for single axis regulation. Pre-control coefficients will be adapted to have more performance. Psychphysical experimentations will be conducted to validate these approches in riding motorcycle aspect.

REFERENCES

S. Chiyoda, K. Yoshimoto, D. Kawasaki, Y. Murakami, and T. Sugimoto. Development of a motorcycle simulator using parallel manipulator and head mounted display. In *Driving Simulation Conference(DSC00)*, Paris,France, 2000.

V. Cossalter. *Motorcycle Dynamics*. Race Dynamics Inc, ISBN: 0-9720514-0-6, Milwaukee, USA, 2002.

V. Cossalter, A. Doria, and R. Lot. Development and validation of a motorcycle riding simulator. In *World Automotive Congress(FISITA2004)*, Barcelona, Spain, May 2004.

B. Dasgupta and T.S. Mruthyunjaya. Closed-form dynamic equations of the general stewart platform through the newton-euler approach. *Mech. Mach.Theory*, 33:993–1012, 1998.

D. Ferrazzin, F. Barnagli, C.A. Avizzano, G.Di Pietro, and M. Bergamasco. Designing new commercial motorcycles through a highly reconfigurable virtual reality-based simulator. *Journal of Advanced Robotics*, 17(4):293–318, 2003.

Y. Miyamaru, G. Yamasaki, and K. Aoki. Development of a motorcycle riding simulator. *Society of Automotive Engineers of Japan*, 23:121–126, 2002.

L. Nehaoua, H. Arioui, H. Mohellebi, and S. Espié. Restitution Movement for a Low Cost Driving Simulator. In *Proceedings of the 2006 American Control Conference (ACC06)*, pages 2599–2604, Minneapolis, Minnesota, June 2006.

L. Nehaoua, S. Hima, H. Arioui, N. Seguy, and S. Espie. Design and modeling of a new motorcycle riding simulator. *American Control Conference (ACC07)*, pages 171–181, 2007.